

Synthesis and Optical Properties of Colloidal Tungsten Oxide Nanorods

Kwangyeol Lee, Won Seok Seo, and Joon T. Park*

National Research Laboratory, Department of Chemistry and School of Molecular Science (BK 21),
Korea Advanced Institute of Science and Technology (KAIST), Daejeon 305-701, Korea

Received January 2, 2003; E-mail: jtpark@mail.kaist.ac.kr

Nanostructured materials are expected to play a crucial role in the future technological advance in electronics,¹ optoelectronics,² and memory devices.³ One-dimensional nanostructures in particular offer fundamental opportunities for investigating the effect of size and dimensionality on their collective optical, magnetic, and electronic properties. Various 1-D nanostructured metal oxides have been obtained via several different synthetic approaches, including solvothermal methods,⁴ template-directed syntheses,⁵ sonochemistry,⁶ thermal evaporation,⁷ and gas-phase catalytic growth.⁸ Control over the dimension of the prepared nanocrystals, however, is rarely accomplished due to the required harsh reaction conditions. Controlled colloidal nanocrystal growth under mild conditions in the presence of structure-directing surfactants has attracted much attention due to flexible processing chemistry in terms of solubility and nanocrystal dimension and has been successfully applied for a number of metals⁹ and metal chalcogenides.¹⁰ However, its application to the growth of 1-D metal oxide is extremely rare.¹¹

Among various metal oxides, WO_{3-x} has found useful applications in electrochromic devices,¹² semiconductor gas sensors,¹³ and photocatalyses.¹⁴ Sodium-doped WO_3 is also reported to be a high-temperature superconductor with $T_c \approx 90$ K.¹⁵ In addition, one-dimensional nanostructured tungsten oxide has been used as a structure-directing precursor for WS_2 nanotube,¹⁶ a useful material in tribological applications and catalyses; the dimension of oxide nanorod is directly transferred to the resulting WS_2 nanotube after reaction with $\text{H}_2/\text{H}_2\text{S}$. Thus far, preparation of single-crystalline, 1-D nanostructured tungsten oxide in mass quantity has been accomplished by heating a tungsten foil, covered by SiO_2 plate, in an argon atmosphere at 1600 °C¹⁷ or recently by electrochemically etching a tungsten tip, followed by heating at 700 °C under argon.¹⁸ The employed harsh conditions, contamination by platelets, and uncontrolled size hamper systematic investigations on size-dependent properties of the oxide nanorod itself as well as of inorganic derivatives prepared from the oxide. Herein we report a simple large-scale preparation of soluble and highly crystalline tungsten oxide nanorods of varying sizes by a mild, solution-based colloidal approach.

A stirred slurry of 0.70 g of $\text{W}(\text{CO})_6$ (Strem, 99%), 1.33 g of $\text{Me}_3\text{NO} \cdot 2\text{H}_2\text{O}$ (6 equiv, Aldrich, 98%), and 8.5 g of oleylamine (16 equiv, Aldrich, 70% (technical grade)) in a 100-mL Schlenk tube, connected to a gas bubbler, was slowly heated in an oil bath from room temperature to 270 °C over 2 h. Over the course of the reaction, a vigorous frothing was observed, accompanied by a series of color changes from brown, bluish green, pink, to white. Gas evolution subsided at the bath temperature of 250 °C, and the reaction mixture became a clear, deep-green solution. The reaction mixture became a viscous, deep-blue-colored oil at the bath temperature of 270 °C, and was further aged at the same temperature for 24 h. The cooled viscous blue oil was diluted with toluene (20 mL), and to the resulting blue solution was added ethanol (50 mL) to form a blue precipitate. Centrifugation, redissolution in toluene,

and precipitation by ethanol gave a blue powder, which can be easily redispersed in various solvents such as dichloromethane, toluene, and chlorobenzene.¹⁹

The structure of the product was examined with transmission electron microscopy (Omega EM912 operated at 120 kV) and high-resolution transmission electron microscopy (HRTEM; Philips F20Tecnai operated at 200 kV).²⁰ A rodlike morphology with average diameter of 4 ± 1 nm and average length of 75 ± 20 nm (aspect ratio ≈ 20) is observed as shown in Figure 1a. The diameter of nanorods is uniform throughout their length. The selected area electron diffraction (SAED) as shown in Figure 1b exhibits two intense rings corresponding to lattice spacings of 3.78 Å (inner ring) and 1.89 Å (outer ring), suggesting the preferential rod growth in one direction. The unidirectional growth of the nanorods is clearly shown in the HRTEM image (Figure 1c), and the lattice spacing along the direction of rod growth is found to be 3.78 Å, consistent with the SAED pattern.

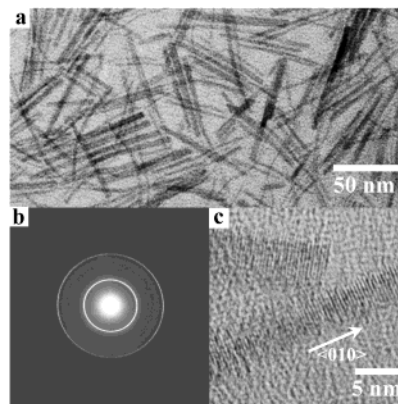


Figure 1. (a) a TEM micrograph of 75 ± 20 nm tungsten oxide nanorods, (b) a selected area electron diffraction pattern (SAED), and (c) a high-resolution TEM image.

The X-ray powder diffraction (XRD, Rigaku D/MAX-RC (12 kW) diffractometer using graphite-monochromatized Cu–K radiation at 40 kV and 45 mA) pattern as shown in Figure 2 gives information about the possible stoichiometry of the prepared tungsten oxide nanorods, and it matches best the $\text{W}_{18}\text{O}_{49}$ reflections (JCPDS card No: 05-0392) among various tungsten oxide systems.

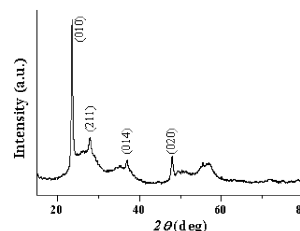


Figure 2. XRD pattern of 75 ± 20 nm tungsten oxide nanorods.

Comparing the intensities of the (010) and (014) peaks of the sample with those of the bulk $W_{18}O_{49}$, it was found that the relative intensity of (010) has been dramatically increased (from 100 to 225%), implying that the nanorod growth occurs along $\langle 010 \rangle$ direction.

The length of the tungsten oxide nanorods can be easily varied by simple changes in the reaction parameters. Shorter nanorods of 25 ± 6 nm in length (aspect ratio ≈ 10) were obtained at the reaction temperature of 250 °C (Figure 3a).¹⁹ Longer nanorods of 130 ± 30 nm in length (aspect ratio ≈ 20) were prepared at 270 °C by using 12 equiv of oleylamine instead of 16 equiv (Figure 3b).¹⁹ At reaction temperatures below 250 °C, no nanorod formation was observed, and contamination by platelets was observed at reaction temperatures above 270 °C. Longer reaction time caused little effects on the lengths of nanorods.

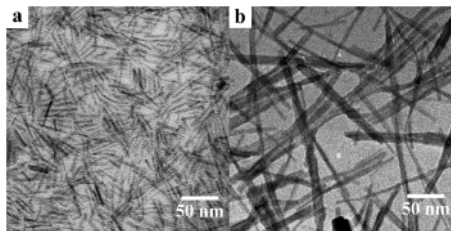


Figure 3. TEM micrographs of (a) 3 ± 0.5 nm \times 25 ± 6 nm and (b) 6 ± 1.5 nm \times 130 ± 30 nm tungsten oxide nanorods.

Little is known about the photoluminescence of nanostructured tungsten oxides.²¹ Figure 4 shows the room-temperature PL emission spectra (Spex Fluorolog-3, 450 W Xe arc-lamp, excitation at 275 nm) of the three tungsten oxide nanorod samples of various lengths dissolved in dichloromethane.

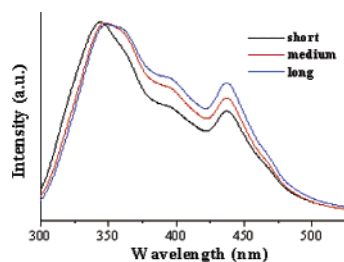


Figure 4. Photoluminescence spectra of tungsten oxide nanorods; 25 ± 6 nm (short), 75 ± 20 nm (medium), and 130 ± 30 nm (long).

The strongest PL emission peaks appear at 3.60 eV (344 nm), 3.56 eV (348 nm), 3.55 eV (349 nm) for short (25 ± 6 nm), medium (75 ± 20 nm), and long (130 ± 30 nm) nanorod samples, respectively. The very weak size-dependency of PL indicates that the prepared tungsten oxide nanorod samples are on the border of the quantum confinement regime. All three PL emission spectra feature an additional blue emission peak at 2.84 eV (437 nm), and the intensity of this peak increases relative to that of UV emission as the length of nanorods increases. A similar PL pattern with two emission maxima, yet at much lower energies of 2.8 and 2.3 eV, was previously observed for thin film of the related WO_3 system at 80 K, but the emission peak at higher energy (2.8 eV) disappeared at room temperature.²² While the higher-energy peak was attributed to an electron–hole radiative recombination, the lower-energy peak was assigned to localized states in the band gap due to impurities.^{22b} In light of these assignments, we suggest that the UV emission of

nanorod samples in this work might correspond to the band-to-band transition. The blue emission of nanorods might originate from the presence of oxygen vacancies or defects; longer nanorods would possess more defects due to faster 1-D crystal growth and thus more intense PL emission associated with the presence of defects. Also, the position of this blue emission peak does not show any size-dependency, presumably, due to its irrelevance to the band structures of the tungsten oxide system.

In summary, we have reported the first solution-based preparation of soluble and highly crystalline tungsten oxide nanorods of varying lengths, which might be easily scaled up, as well as their photoluminescent behaviors at room temperature. The simple and reliable synthetic procedure for a mass quantity of soluble tungsten oxide nanorods would be very useful for practical application of these materials as well as for the preparation of inorganic derivatives such as WS_2 . Preliminary results show that the same synthetic strategy can be applied to obtain nanorods of cobalt oxides, and we are currently investigating the generality of our method for the preparation of soluble 1-D nanostructured metal oxides.

Acknowledgment. This work was supported by the NRL Program of the Korean Ministry of Science & Technology and by the KOSEF (Project No. 1999-1-122-001-5). We thank the staffs of KBSI and KAIST for TEM analyses. We also thank reviewers for helpful comments.

References

- (1) Cui, Y.; Lieber, C. M. *Science* **2001**, *291*, 851.
- (2) Alivisatos, A. P. *Science* **1996**, *271*, 933.
- (3) Sun, S.; Murray, C. B.; Weller, D.; Folks, L.; Moser, A. *Science* **2000**, *287*, 1989.
- (4) Wang, X.; Li, Y. *J. Am. Chem. Soc.* **2002**, *124*, 2880.
- (5) Patzke, G. R.; Krumeich, F.; Nesper, R. *Angew. Chem., Int. Ed.* **2002**, *41*, 2446; See references therein.
- (6) Zhu, Y.; Li, H.; Kolytyn, Y.; Hacothen, Y. R.; Gedanken, A. *Chem. Commun.* **2001**, 2616.
- (7) Pan, Z. W.; Dai, Z. R.; Wang, Z. L. *Science* **2001**, *291*, 1947.
- (8) Hu, J.; Odom, T. W.; Lieber, C. M. *Acc. Chem. Res.* **1999**, *32*, 435.
- (9) (a) Jana, N. R.; Gearheart, L.; Murphy, C. J. *Chem. Commun.* **2001**, 617. (b) Dumestre, F.; Chaudret, B.; Amiens, C.; Fromen, M.-C.; Casanove, M.-J.; Renaud, P.; Zurcher, P. *Angew. Chem., Int. Ed.* **2002**, *41*, 4286.
- (10) (a) Lee, S.-M.; Jun, Y.-W.; Cho, S.-N.; Cheon, J. *J. Am. Chem. Soc.* **2002**, *124*, 11244. (b) Peng, X.; Manna, L.; Yang, W.; Wickham, J.; Scher, E.; Kadavanich, A.; Alivisatos, A. P. *Nature* **2000**, *404*, 59.
- (11) (a) Guo, L.; Ji, Y. L.; Xu, H.; Simon, P.; Wu, Z. *J. Am. Chem. Soc.* **2002**, *124*, 14864. (b) Urban, J. J.; Yun, W. S.; Gu, Q.; Park, H. *J. Am. Chem. Soc.* **2002**, *124*, 1186.
- (12) Santato, C.; Odziemkowski, M.; Ulmann, M.; Augustynski, J. *J. Am. Chem. Soc.* **2001**, *123*, 10639.
- (13) Solis, J. L.; Saukko, S.; Kish, L.; Granqvist, C. G.; Lantto, V. *Thin Solid Films* **2001**, *391*, 255.
- (14) Sayama, K.; Mukasa, K.; Abe, R.; Abe, Y.; Arakawa, H. *Chem. Commun.* **2001**, 2416.
- (15) Shengelaya, A.; Reich, S.; Tsabba, Y.; Müller, K. A. *Eur. Phys. J. B* **1998**, *12*, 13.
- (16) Rothschild, A.; Sloan, J.; Tenne, R. *J. Am. Chem. Soc.* **2000**, *122*, 5169.
- (17) Zhu, Y. Q.; Hu, W.; Hsu, W. K.; Terrones, M.; Grobert, N.; Hare, J. P.; Kroto, H. W.; Walton, D. R. M.; Terrones, H. *Chem. Phys. Lett.* **1999**, *309*, 327.
- (18) Gu, G.; Zheng, B.; Han, W. Q.; Roth, S.; Liu, J. *Nano Lett.* **2002**, *2*, 849.
- (19) The toluene or chlorobenzene colloidal solutions of all three samples of freshly prepared tungsten oxide nanorods are stable for several days at room temperature, while CH_2Cl_2 solutions are stable only for several hours. No discernible difference in solubility was observed for the three samples.
- (20) Samples for TEM investigations were prepared by transferring an aliquot of toluene solution of $W_{18}O_{49}$ or $WO_{2.72}$ nanorods onto an amorphous carbon substrate supported on a copper grid.
- (21) Niederberger, M.; Bartl, M. H.; Stucky, G. D. *J. Am. Chem. Soc.* **2002**, *124*, 13642.
- (22) (a) Manfredi, M.; Paracchini, G. C.; Schianchi, G. *Thin Solid Films* **1981**, *79*, 161. (b) Paracchini, C.; Schianchi, G. *Phys. Status Solidi A* **1982**, *72*, K129.

JA034011E